

Electron-impact excitation autoionization of Ga II

M. S. Pindzola

Department of Physics, Auburn University, Auburn, Alabama 36849

D. C. Griffin* and C. Bottcher

Physics Division, Oak Ridge National Laboratory, Oak Ridge, Tennessee 37830

(Received 14 August 1981)

The general-reaction theory of Feshbach is applied, within the framework of the distorted-wave approximation, to the calculation of excitation-autoionization resonances in the electron-impact ionization of Ga^+ . Although the spectrum of autoionizing levels for Ga^+ is quite complex, we focus our attention on the important $3d^{10}4s^2 \rightarrow 3d^9 4s^2 4p$ inner-shell excitations. For excitation of the $3d^9 4s^2 4p \ ^1P_1$ autoionizing level we make a general-reaction-theory calculation for the dominant partial-wave cross section and compute a typical resonance profile in the ejected-electron differential cross section. We find that the quantum-mechanical interference between the direct and indirect processes has a small effect on the total ionization cross section. Employing an independent-processes approximation we calculate excitation-autoionization contributions to all twelve levels of the $3d^9 4s^2 4p$ configuration. Using the results of our calculations and their comparison with a recent crossed-beam experiment by Rogers *et al.*, we discuss the accuracy of the distorted-wave method and the effects of configuration interaction on energy levels and excitation cross sections.

I. INTRODUCTION

Among many applications, the knowledge of electron-impact ionization cross sections for atomic ions is of importance to the understanding of the heating and cooling processes in high temperature plasmas. A significant contribution to the total ionization cross section may come from the excitation of an inner-subshell electron to a bound state lying above the first ionization limit, followed by autoionization. The first experimental confirmation that the excitation-autoionization enhancement can be quite large came from crossed-beam experiments on the singly charged ions Mg^+ , Ca^+ , Sr^+ , and Ba^+ .¹ Of this group the most dramatic result is the fourfold resonant enhancement in the total ionization cross section found for Ba^+ by Peart *et al.*² and Feeney *et al.*³ Crossed-beam measurements have also been made on various multiply-charged atomic ions. For C^{3+} , N^{4+} , and O^{5+} , Crandall *et al.*⁴ found that excitation autoionization makes a 10 to 30% contribution to the total ionization cross section. Quite recently Falk *et al.*⁵ have found resonant enhancements in Ti^{3+} , Zr^{3+} , and Hf^{3+} which are much larger than in Ba^+ .

A simple theoretical approach to the calculation of electron-impact ionization cross sections is to assume that direct ionization and excitation autoionization are independent processes. To allow for resonance decay by radiative processes, branching ratios must also be introduced. Calculations for the direct process are made in a variety of ways, e.g., the Lotz semiempirical formula,⁶ the scaled hydrogenic model of Golden and Sampson,⁷ the Coulomb-Born approximation,⁸ and the distorted-wave approximation.⁹ Crude estimates for the indirect process may be made by calculating excitation cross sections using the effective Gaunt factor^{10,11} and by assuming unit branching ratios. More accurate estimates rely on distorted-wave excitation cross sections and realistic branching ratios as found, for example, in the recent study by Cowan and Mann.¹² In response to the experiments by Crandall *et al.*,⁴ excitation cross sections to autoionization levels for various Li-like ions have now been calculated in the Coulomb-Born with exchange,¹³ distorted-wave,^{14,15} and close-coupling approximations.¹⁶

A general theoretical approach to the problem of electron-impact ionization should include the quantum-mechanical interference between the

direct and indirect processes. For many years the formalism of Fano¹⁷ has been applied to study the fast electron excitation of autoionizing states in neutral atoms.¹⁸ Jakubowicz and Moores¹⁹ have recently calculated ionization cross sections of Li-like and Be-like atomic ions taking interference into account in their Coulomb-Born method by using close-coupling wave functions to represent the initial and final states of the target system. In Sec. II of this paper we apply the general-reaction theory of Feshbach,²⁰ within the framework of the distorted-wave approximation, to calculate excitation-autoionization resonances in the electron-impact ionization of atomic ions. The theoretical formulation is similar in spirit to recent work on radiative recombination²¹ and electron-impact excitation.²² In Sec. III we make a model calculation for the electron ionization of Ga⁺ using the general-reaction theory. We focus our attention on the important $3d^9 4s^2 4p^1 P_1$ autoionizing level and compute a typical resonance profile in the ejected-electron differential cross section. We find that interference between the direct and indirect processes has a small effect on the total ionization cross section. In Sec. IV we employ the simpler independent processes theory to calculate excitation-autoionization contributions to all 12 levels of the $3d^9 4s^2 4p$ configuration. We compare our results with a recent crossed-beam experiment by Rogers *et al.*²³ and discuss the accuracy of the distorted-wave method and the effects of configuration interaction on energy levels and excitation cross sections.

II. THEORY

The general theory for electron-impact ionization of atomic ions in the distorted-wave approximation is quite well known.²⁴ The total ionization cross section σ , in atomic units, is given by

$$\sigma = \sum_{LSl_i l_f} \sum_{L_f S_f l_e} \sigma(l_i \rightarrow l_f, LS, L_f S_f l_e), \quad (1)$$

where

$$\begin{aligned} \sigma(l_i \rightarrow l_f, LS, L_f S_f l_e) &= \int_0^{E_{\max}} \frac{d\sigma}{d\epsilon}(l_i \rightarrow l_f, LS, L_f S_f l_e) d\epsilon, \quad (2) \\ \frac{d\sigma}{d\epsilon}(l_i \rightarrow l_f, LS, L_f S_f l_e) &= \frac{16}{k_i^2} \frac{(2L+1)(2S+1)}{(2L_i+1)(2S_i+1)} |M_{fi}|^2, \quad (3) \end{aligned}$$

and

$$M_{fi} = \langle \Psi(\beta L_e L_f S_f LS) | H - E | \Psi(\alpha L_i S_i LS) \rangle. \quad (4)$$

We assume that the total orbital and spin angular-momentum quantum numbers LS , as well as parity, are conserved during the collision. The linear momenta \vec{k}_i , \vec{k}_f , and \vec{k}_e and the angular-momentum quantum numbers l_i , l_f , and l_e correspond to the incoming, outgoing, and ejected electron, respectively. The ejected-electron energy $\epsilon = k_e^2/2$ reaches a maximum energy E_{\max} given by

$$E_{\max} = \frac{k_i^2}{2} - I = \frac{k_e^2}{2} + \frac{k_f^2}{2}, \quad (5)$$

where I is the ionization potential of the N -electron target ion. The quantum numbers $L_i S_i$ and $L_f S_f$ correspond to the initial and final states of the target ion, respectively.

The initial $(N+1)$ -electron atomic state $\Psi(\alpha L_i S_i LS)$ may be chosen to be an LS coupled antisymmetrized product of a particular N -electron target ion state $\Phi(\alpha L_i S_i)$ and an incoming continuum orbital F_i . Our notation for this product will be $[\Phi(\alpha L_i S_i), F_i; LS]$. Similarly the final $(N+1)$ -electron atomic state $\Psi(\beta L_f S_f LS)$ may be chosen equal to $[\Phi(\beta L_f S_f), F_f; LS]$. In lowest order of perturbation theory the final N -electron target ion state $\Phi(\beta L_f S_f)$ is given by $[\theta(\gamma L_e S_e), F_e; L_f S_f]$, where $\theta(\gamma L_e S_e)$ is an $(N-1)$ -electron residual ion state.

In the distorted-wave approximation the continuum orbital $F = P_{kl}(r) Y_{lm}(\theta, \phi) \chi_{m_s}$ is found by solving

$$\left[\frac{d^2}{dr^2} - \frac{l(l+1)}{r^2} + \frac{2Z}{r} - 2V + k^2 \right] P_{kl}(r) = 0, \quad (6)$$

where Z is the atomic number of the target ion and V in the Hartree-Fock approximation symbolizes both direct and nonlocal exchange potential terms. The continuum normalization is chosen such that

$$P_{kl}(r) \xrightarrow{r \rightarrow \infty} \frac{1}{\sqrt{k}} \sin \left[kr + \frac{q}{k} \ln(2kr) - \frac{l\pi}{2} + \delta_l \right], \quad (7)$$

where $q = Z - N$ and δ_l is the phase shift.

We may improve our description of the electron-impact ionization process by applying general-reaction theory²⁰ to the final N -electron target ion state $\Phi(\beta L_f S_f)$. In this manner we will

incorporate the interaction between an N -electron autoionization state and the ejected-electron continuum. The wave function may be divided into two parts

$$\Phi(\beta L_f S_f) = P\Phi(\beta L_f S_f) + Q\Phi(\beta L_f S_f), \quad (8)$$

where P is an open-channel projection operator and Q is a closed-channel projection operator. Through first order a formal solution of Schrödinger's equation leads to the uncoupled equation

$$P\Phi(\beta L_f S_f) = P\psi(\beta L_f S_f), \quad (9)$$

$$Q\Phi(\beta L_f S_f) = \sum_n \frac{Q\Phi(nL_f S_f) \langle Q\phi(nL_f S_f) | \mathcal{H} - \mathcal{E} | P\psi(\beta L_f S_f) \rangle}{\mathcal{E} - \mathcal{E}_n + \frac{iW_n}{2}}, \quad (10)$$

where

$$(P\mathcal{H}P - \mathcal{E})P\psi(\beta L_f S_f) = 0, \quad (11)$$

$$(Q\mathcal{H}Q - \mathcal{E}_n)Q\phi(nL_f S_f) = 0, \quad (12)$$

and \mathcal{H} is the N -electron Hamiltonian. The resonance energy \mathcal{E}_n and total width W_n correspond to the n th autoionization state $Q\phi(nL_f S_f)$. Coupling to the radiation field introduces additional radiative forms in W_n . The Hamiltonian matrix element of Eq. (4) may now be written as

$$M_{fi} = \tilde{M}_{fi} + \sum_n \frac{A_n X_{fi}}{\mathcal{E} - \mathcal{E}_n + \frac{iW_n}{2}}, \quad (13)$$

where

$$\tilde{M}_{fi} = \langle [P\psi(\beta L_f S_f), F_f; LS] | H - E | [\Phi(\alpha L_i S_i), F_i; LS] \rangle, \quad (14)$$

$$A_n = \langle P\psi(\beta L_f S_f) | \mathcal{H} - \mathcal{E} | Q\phi(nL_f S_f) \rangle, \quad (15)$$

and

$$X_{fi} = \langle [Q\phi(nL_f S_f), F_f; LS] | H - E | [\Phi(\alpha L_i S_i), F_i; LS] \rangle. \quad (16)$$

The functions $P\psi(\beta L_f S_f)$ and $Q\phi(nL_f S_f)$ cannot be calculated exactly for a many-electron target.

We thus make the approximations that $P\psi(\beta L_f S_f) = [\theta(\gamma L_e S_e), F_e; L_f S_f]$ and that $Q\phi(nL_f S_f)$ is an autoionization state calculated in some standard atomic model.²²

Upon substitution of Eq. (13) into Eq. (3) the differential cross section, $d\sigma/d\epsilon$, is now seen to contain resonance structures analogous to those found in photoionization theory. The total ionization cross section as a function of incident energy will appear as a series of steps as the various autoionization levels become energetically accessible. We may improve our electron ionization description further by going to even higher-order perturbation theory. By applying general-reaction theory to the initial $(N+1)$ -electron atomic state, $\Psi(\alpha L_i S_i LS)$, we may include the process of electron capture to an autoionization state of the total system. This state may then sequentially decay with the emission of two electrons.²⁵ In certain

cases higher-order terms may significantly alter the $d\sigma/d\epsilon$ resonance profiles in a manner analogous to the perturbation-theory treatment of photoabsorption window resonances in argon.²⁶

From our first-order general-reaction theory results we may easily recover the independent processes form of the total ionization cross section. We simply assume that the matrix elements of Eqs. (14)–(16) are only weakly dependent on energy and then average over each resonance in turn. The total cross section of Eq. (1) reduces to the well-known result

$$\sigma = \tilde{\sigma} + \sum_m \frac{\Gamma_m}{W_m} \sigma_x^m, \quad (17)$$

where the summation over m includes the entire spectrum of autoionization states, i.e., all values of L_f and S_f that are allowed. The direct-ionization cross section $\tilde{\sigma}$ is found from Eqs. (1)–(4) upon substitution of \tilde{M}_{fi} of Eq. (14) for M_{fi} . The excitation cross section σ_x^m to the various autoioniza-

tion states is given by

$$\sigma_x^m = \sum_{LSl_i l_f} \sigma_x^m(l_i \rightarrow l_f, LS), \quad (18)$$

where

$$\sigma_x^m(l_i \rightarrow l_f, LS) = \frac{8\pi(2L+1)(2S+1)}{k_i^2(2L_i+1)(2S_i+1)} |X_{fi}|^2. \quad (19)$$

The quantity Γ_m/W_m in Eq. (17) is the autoionization branching ratio, where the autoionization width Γ_m is given by

$$\Gamma_m = 4 |A_m|^2. \quad (20)$$

III. MODEL CALCULATION FOR Ga II

The photoionization cross section for the 4s subshell of the neutral Zn atom, which is isoelectronic with Ga^+ , is dominated near threshold by autoionization resonances due to the $3d^9 4s^2 4p$ configuration.²⁷ There are six multiplets and 12 levels arising from the $3d^9 4s^2 4p$ configuration. Due to the spin-orbit interaction all three levels 1P_1 , 3P_1 , and 3D_1 can be excited optically from the ground state. Since electron-impact excitation is not limited by optical selection rules, it is possible to excite all 12 levels. Recent electron ionization experiments^{28,29} have identified structures in the ionization efficiency curve of Zn which can be attributed to many of the 12 levels. A number of lines were assigned to additional members of the $3d^9 4s^2 np$ and $3d^9 4s^2 nf$ series. Lines resulting from the simultaneous excitation of both 4s electrons were also observed.

In this section we focus our attention on the $3d^9 4s^2 4p \ ^1P_1$ resonance level and make a model calculation based on the general-reaction theory of Sec. II. We calculated the ground and inner-shell excited bound states of Ga^+ in a single configuration Hartree-Fock (HF) approximation.³⁰ Our HF energies are given in the first row of Table I. For Ga^+ the $3d^9 4s^2 4p \ ^1P_1$ level is autoionizing at 2.3 eV above the 4s subshell ionization limit. An intermediate coupling calculation using first-order perturbation theory shows that the $3d^9 4s^2 4p \ ^1P_1$ level is 94% pure, having a 3% mixture of 3P_1 and a 3% mixture of 3D_1 . We thus treat the $3d^9 4s^2 4p \ ^1P_1$ level as a single LS term in the following model calculation.

The $3d^9 4s^2 4p \ ^1P_1$ electron-impact excitation cross section for Ga^+ was calculated in the distorted-wave approximation using Eqs. (18) and (19). Standard algebraic methods were employed to reduce the Hamiltonian matrix element of Eq. (16) to radial quadrature. The continuum orbitals were obtained by solving Eq. (6) in the Hartree-Fock approximation.³¹ Both incoming and outgoing waves were calculated in the distorting potential V of the ground $3d^{10} 4s^2 \ ^1S$ state in order to simplify orthogonality conditions. For an incident energy of 22 eV, which lies 3.5 eV above the single-configuration Hartree-Fock 4s ionization limit and 1.2 eV above the threshold for excitation of the $3d^9 4s^2 \ ^1P_1$ level, we found the cross section to be $26.8 \times 10^{-18} \text{ cm}^2$. The two largest partial-wave cross sections are $\sigma_x(d \rightarrow p, \ ^2D) = 10.3 \times 10^{-18} \text{ cm}^2$ and $\sigma_x(f \rightarrow d, \ ^2F) = 12.2 \times 10^{-18} \text{ cm}^2$.

TABLE I. Ga^+ energies.

Method	Ionization potential (eV)	$3d^9 4s^2 4p$ Center of gravity (eV)	$3d^9 4s^2 4p \ ^1P_1$ (eV)
Hartree-Fock (HF)	18.5	20.3	20.8
Hartree-Fock Relativistic (HFR)	18.8	19.6	20.1
Hartree-Fock Relativistic with 4s pair correlations (HFRs)	19.7	19.6	20.1
Hartree-Fock Relativistic with 4s and 3d pair correlations (HFRsd)	19.7	22.3	22.8

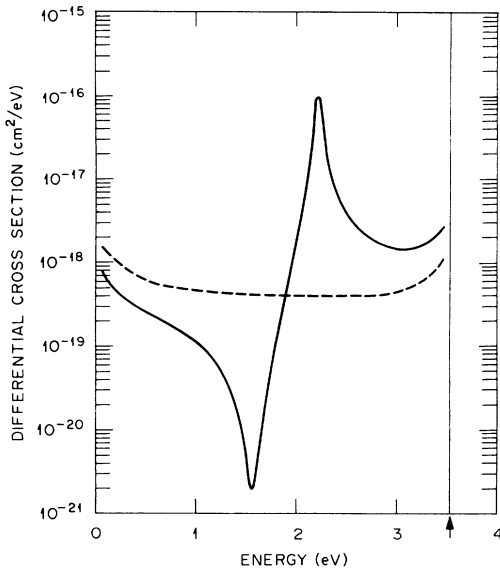


FIG. 1. Partial-wave differential cross section for Ga^+ ; $d\sigma/d\epsilon(f \rightarrow d, {}^2F, {}^1Pp)$. The incident energy is 22.0 eV, which lies 3.5 eV above the single-configuration Hartree-Fock 4s ionization limit and 1.2 eV above the threshold for excitation of the $3d^9 4s^2 4p \ ^1P_1$ level. — — —, direct-ionization differential cross section; —, total ionization differential cross section including $3d^9 4s^2 4p \ ^1P_1$ resonance.

We applied the general-reaction theory of Sec. II to calculate the $d\sigma/d\epsilon(f \rightarrow d, {}^2F, {}^1Pp)$ partial-wave differential cross section at 22-eV incident energy. A plot of cross section versus ejected-electron energy is shown in Fig. 1 as the solid curve. We again used Hartree-Fock energies and bound orbitals. The incoming and outgoing continuum orbitals were calculated in the potential of the ground $3d^{10} 4s^2 \ ^1S$ state while the ejected wave was calculated in the field of the $3d^{10} 4s^2 \ ^2S$ residual ion. The $3d^9 4s^2 4p \ ^1P_1$ autoionization width was found to be 0.083 eV or 1.26×10^{14} Hz. The branching ratio is thus very close to unity. The $d\bar{\sigma}/d\epsilon(f \rightarrow d, {}^2F, {}^1Pp)$ differential cross section, whose contributions are due to direct ionization only, is shown in Fig. 1 as the dashed curve. Upon integration over the ejected-electron spectrum, $\bar{\sigma}(f \rightarrow d, {}^2F, {}^1Pp) = 2.2 \times 10^{-18} \text{ cm}^2$ and $\sigma(f \rightarrow d, {}^2F, {}^1Pp) = 13.8 \times 10^{-18} \text{ cm}^2$. We may also use Eq. (17) and the previously calculated value for $\sigma_x(f \rightarrow d, {}^2F) = 12.2 \times 10^{-18} \text{ cm}^2$ to find that $\sigma(f \rightarrow d, {}^2F, {}^1Pp) = 14.4 \times 10^{-18} \text{ cm}^2$ in the independent-processes approximation. We thus conclude that the quantum-mechanical interference between the direct and indirect processes has a small effect on the largest partial-wave cross section. We expect similar quantitative results for

other partial waves involving the excitation of the $3d^9 4s^2 4p \ ^1P_1$ resonance.

From our model calculation for Ga^+ we predict that effects on the total ionization cross section arising from interference between the two terms in Eq. (13) will be most noticeable in the immediate vicinity of the autoionization steps. The general-reaction theory modifies the step profile to take into account the onset of an autoionization resonance with a finite width. Interference effects will in general be unobservable if experimental beam spreads exceed the resonance widths.

IV. GENERAL CALCULATION FOR $\text{Ga} \text{ II}$

The results of Sec. III indicate that interference between the direct and indirect processes has a small effect on the total ionization cross section. In this section we will thus use the independent-processes approximation given by Eq. (17) to calculate the total ionization cross section for Ga^+ .

We use both the semiempirical formula of Lotz⁶ and the scaled-plane-wave Born (PWB) calculations of McGuire³² to estimate the direct-ionization cross section. The Lotz formula is known to overestimate the contribution of the direct process in many cases, and Rogers *et al.*²³ have shown that it overestimates $\bar{\sigma}$ of Eq. (17) for Zn^+ at low energies before the onset of the indirect process, as well as at high energies for both Zn^+ and Ga^+ . As such, the Lotz equation provides an upper limit to the direct-ionization cross section. The PWB results may provide a better estimate of $\bar{\sigma}$ in Ga^+ since it agrees quite well with experiment in Zn^+ before the onset of the indirect process.

In calculating the contributions of excitation autoionization for Ga^+ , it is especially important to calculate the energies of the quasibound states accurately. The contribution of indirect ionization appears from experiment²³ to become quite large within a few electron volts of the ionization threshold; thus the lowest autoionization levels are near the ionization edge and the indirect cross section will be very sensitive to the position of these levels relative to the $3d^{10} 4s^2$ ground state of Ga^{2+} .

In this section we consider the contributions of excitations to all 12 levels of the $3d^9 4s^2 4p$ configuration. As previously mentioned the HF values of the ionization potential, the center of gravity of $3d^9 4s^2 4p$ and the $3d^9 4s^2 4p \ ^1P_1$ level are shown in the first row of Table I. The HF ionization poten-

tial of 18.5 eV differs substantially from the experimental value of 20.5 eV, and the position of the $3d^9 4s^2 4p$ appears to be too low, being nearly equal to the experimental ionization energy. We included relativistic effects by using the Hartree-Fock method with relativistic modifications (HFR),³³ which includes the mass velocity and Darwin corrections within modified HF differential equations. This provides a small improvement on the ionization potential but lowers the position of the $3d^9 4s^2 4p$ configuration. These results were checked by performing a Dirac-Fock calculation³⁴ and we found that the HFR energies are within 0.1 eV of the fully relativistic results.

The effects of electron correlation should be substantial in Zn-like ions. We approximated the $4s$ pair correlation in the ground-state configuration $3d^{10} 4s^2$ by performing a multiconfiguration Hartree-Fock (MCHF) calculation³⁰ on $3d^{10} 4s^2$ plus $3d^{10} 4p^2$. We found that the $3d^{10} 4s^2$ configuration was lowered by 0.9 eV. If we assume that the $4s$ pair correlation is the same in $3d^9 4s^2 4p$, this effect increases the ionization potential, but does not affect the position of the $3d^9 4s^2 4p$ configuration. This estimate is designated by HFRs in Table I. It is well known that pair correlation within the $3d^{10}$ subshell is very large.^{35,36} For example, Jankowski *et al.*³⁶ have determined that the total correlation energy in the $3d^{10}$ subshell of Zn^{2+} is -13.673 eV (or -0.3038 eV per $3d-3d$ pair), and that this value is nearly independent of nuclear charge. If we assume the same correlation per $3d-3d$ pair in $Ga^+ 3d^{10} 4s^2$ and $3d^9 4s^2 4p$, we obtain a correction of 2.73 eV for the energy difference between these two configurations. This

correction, which does not affect the ionization potential, is designated by HFRsd in Table I. It should be noted that if we add this same correction to the HF ionization potential for $Cu^+ 3d^{10}$, we obtain a value within 0.2% of experiment. This method of correcting for correlation effects, however, does not include the differences in pair correlation between nonequivalent electrons. The remaining error in the ionization potential is presumably due to additional correlation effects, such as $3d-4s$ pair correlation. We have used the experimental ionization potential in estimating and plotting the direct-ionization cross section.

The excitation cross sections for $3d^{10} 4s^2 {}^1S_0 \rightarrow 3d^9 4s^2 4p L_m S_m J_m$ were calculated in the distorted-wave approximation using Eqs. (18) and (19) modified for intermediate coupling. We used HFR bound orbitals and the continuum orbitals were obtained by solving Eq. (6) using a semiclassical exchange term.³⁷ This exchange term simplifies the solution of the differential equations and gives results in close agreement with results obtained from the HF distorted-wave program. In calculating the Hamiltonian matrix element of Eq. (16) we included the term which results from the lack of orthogonality between the bound state orbital of the active electron and the continuum orbitals with equal values of angular momentum. The form of this term used in the present calculations is the same as that employed by Clark *et al.*³⁸ It proved to have a significant effect on the cross sections for all transitions except the strong optically allowed excitation to $3d^9 4s^2 4p {}^1P_1$.

The results of our excitation cross section calculations are summarized in Table II. The energies

TABLE II. $Ga^+ 3d^{10} 4s^2 \rightarrow 3d^9 4s^2 4p$ excitation cross sections.

Resonance energy (eV)	Eigenvectors	Cross section (10^{-18} cm ²) at threshold
21.6	$-0.99^3 P_2 + 0.15^3 D_2$	1.5
21.9	$-0.98^3 P_1 + 0.13^3 D_1 - 0.16^1 P_1$	1.4
21.9	$-0.83^3 F_3 - 0.54^1 F_3 + 0.17^3 D_3$	2.5
22.0	$-1.00^3 F_4$	3.5
22.1	$-1.00^3 P_0$	0.3
22.2	$-0.95^3 F_2 + 0.25^3 D_2 + 0.17^1 D_2$	1.8
22.4	$0.71^1 F_3 + 0.62^3 D_3 - 0.34^3 F_3$	1.7
22.5	$0.78^1 D_2 + 0.55^3 D_2 + 0.29^3 F_2$	0.7
22.6	$-0.77^3 D_3 + 0.45^1 F_3 - 0.45^3 F_3$	1.5
22.8	$-0.97^1 P_1 + 0.19^3 D_1 + 0.18^3 P_1$	18.5
22.9	$-0.97^3 D_1 - 0.21^1 P_1 - 0.10^3 P_1$	1.2
22.9	$0.78^3 D_2 - 0.61^1 D_2 + 0.11^3 P_2 + 0.11^3 F_2$	0.7

and eigenvectors were calculated using an atomic structure program furnished to us by Cowan.³⁹ The excitation cross sections in intermediate coupling at threshold were determined by extrapolating each cross section calculated at higher energies back to the threshold energy. As expected the transition to the 1P_1 level at 22.8 eV dominates; however, the excitations to the other 11 levels do make an appreciable contribution to the total cross section. It should be noted that the difference between the 1P_1 cross section value of 26.8×10^{-18} cm² in Sec. III and the value of 18.5×10^{-18} cm² from Table II is due primarily to the change in the excitation energy discussed above. The branching ratios for autoionization were calculated using a method similar to that used by Cowan and Mann¹² and were found to be nearly equal to one. Thus, the total cross section is equal to the sum of the direct-ionization and excitation cross sections.

A plot comparing our calculated ionization cross section with experiment²³ is shown in Fig. 2. Our excitation cross sections, when added to the direct-ionization cross section calculated from the Lotz equation, are about 10% higher than experiment at an energy of 30 eV. At least some of this discrepancy is due to the fact that the Lotz equation tends to overestimate the direct-ionization cross section. When we add our cross sections to the PWB calculation, the agreement between

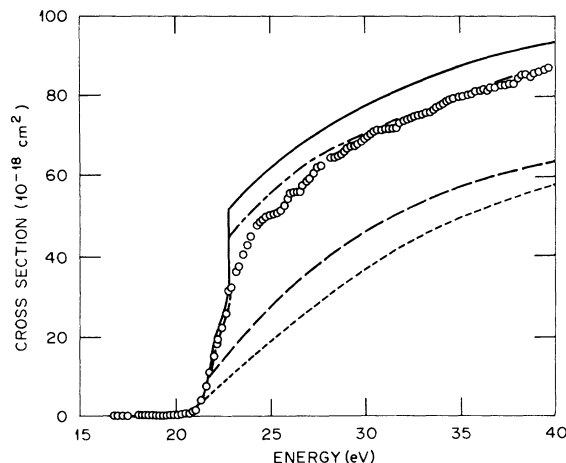


FIG. 2. Total ionization cross section for Ga^+ . — — —, direct-ionization cross section calculated from the Lotz equation; - - - direct ionization calculated from scaled PWB; —, distorted-wave excitation cross section for $3d^{10}4s^2 \rightarrow 3d^9 4s^2 4p$ plus Lotz; - - - —, distorted-wave excitation cross section for $3d^{10}4s^2 \rightarrow 3d^9 4s^2 4p$ plus scaled PWB; O experimental results (Ref. 23).

theory and experiment is excellent.

Despite this apparent agreement, there are reasons to believe that the distorted-wave approximation overestimates the contributions of the $3d^{10}4s^2 \rightarrow 3d^9 4s^2 4p$ transition to the total ionization cross section. We have not included the effects of transitions to the configurations $3d^9 4s^2 nl$ ($nl \neq 4p; n = 4, 5$), which are expected to occur in the energy range from 29 to 35 eV, nor transitions to the doubly excited state $3d^{10} 4p 4d$ which should occur between 21 and 22 eV. Although the contributions of such transitions to the total cross section should be much smaller than the $3d \rightarrow 4p$ excitation, they should still be measurable. In addition, the calculation depicted in Fig. 2 does not include the effects of configuration interaction in the final state of the target ion. The interaction between $3d^9 4s^2 4p$ and the bound-state configuration $3d^{10} 4s 4p$ is particularly important. The excitation cross section for the transition $3d^{10} 4s^2 ^1S_0 \rightarrow 3d^{10} 4s 4p ^1P_1$ is quite large and a small admixture of this state within the eigenvectors of the quasi-bound states will have a significant effect. We have performed a calculation of the cross section for the transition to the quasibound level at 22.8 eV in which we included the configuration mixing between this level and $3d^{10} 4s 4p ^1P_1$. Although the mixing coefficient was only -0.091 , the cross section at threshold increased from 18.5×10^{-18} cm² to 26.6×10^{-18} cm². We found that the $3d^{10} 4s 4p \rightarrow 3d^9 4s^2 4p$ mixing had a small effect on the cross section to other J levels of $3d^9 4s^2 4p$, and the enhancement of the total cross section is approximately 25% near threshold.

Finally our calculations do not explain the rather gradual increase in the experimental cross section between 23 and 28 eV, nor the small but visible structure in this region. However, despite the above mentioned discrepancies, the excitation-autoionization contributions in Ga^+ appear to be reasonably well explained by the distorted-wave method and the independent processes approximation.

ACKNOWLEDGMENTS

We would like to thank W. T. Rogers and G. H. Dunn for providing us with their experimental data prior to publication. We also wish to thank R. D. Cowan for making his atomic structure program available to us and to acknowledge Y. Hahn, C. F. Fisher, S. M. Younger, and D. H. Crandall

for a number of useful conversations. The first author would like to acknowledge partial financial support for this work through a DOE-ORAU Summer Faculty Research Grant at Oak Ridge

National Laboratory. This work was also supported in part by the Office of Fusion Energy, U.S. Department of Energy under contract W-7405-eng-26 with the Union Carbide Corporation.

-
- *On sabbatical leave from Rollins College, Winter Park, Florida.
- ¹K. T. Dolder and B. Peart, *Rep. Prog. Phys.* **39**, 693 (1976).
- ²B. Peart and K. T. Dolder, *J. Phys.* **B1**, 872 (1968); B. Peart, J. G. Stevenson, and K. T. Dolder, *J. Phys. B* **6**, 146 (1973).
- ³R. K. Feeney, J. W. Hooper, and M. T. Elford, *Phys. Rev. A* **6**, 1469 (1972).
- ⁴D. H. Crandall, R. A. Phaneuf, and P. O. Taylor, *Phys. Rev. A* **18**, 1911 (1978); D. H. Crandall, R. A. Phaneuf, B. E. Hasselquist, and D. C. Gregory, *J. Phys. B* **12**, L249 (1979).
- ⁵R. A. Falk, G. H. Dunn, D. C. Griffin, C. Bottcher, D. C. Gregory, D. H. Crandall, and M. S. Pindzola, *Phys. Rev. Lett.* **47**, 494 (1981).
- ⁶W. Lotz, *Z. Phys.* **216**, 241 (1968); *Z. Phys.* **220**, 466 (1969).
- ⁷L. B. Golden and D. H. Sampson, *J. Phys. B* **10**, 2229 (1977).
- ⁸D. L. Moores and H. Nussbaumer, *J. Phys. B* **3**, 161 (1970).
- ⁹S. M. Younger, *Phys. Rev. A* **22**, 111 (1980).
- ¹⁰M. J. Seaton, *Atomic and Molecular Processes* (Academic, New York, 1962), Chap. 11.
- ¹¹H. VanRegemorter, *Astrophys. J.* **136**, 906 (1962).
- ¹²R. D. Cowan and J. B. Mann, *Astrophys. J.* **232**, 940 (1979).
- ¹³D. H. Sampson and L. B. Golden, *J. Phys. B* **12**, L785 (1979).
- ¹⁴N. H. Magee, J. B. Mann, A. L. Merts, and W. D. Robb, Report No. LASL-6691-MS, 1977 (unpublished).
- ¹⁵Y. Hahn, *Phys. Lett.* **78A**, 57 (1980).
- ¹⁶R. J. W. Henry, *J. Phys. B* **12**, L309 (1979).
- ¹⁷U. Fano, *Phys. Rev.* **124**, 1868 (1961).
- ¹⁸V. V. Balashov, A. N. Grum-Grzhimailo, N. M. Kabachnik, A. I. Magunov, and S. I. Strakhova, *Coherence and Correlation in Atomic Collisions* (Plenum, New York, 1980), pp. 283–295.
- ¹⁹H. Jakubowicz and D. L. Moores, *J. Phys. B* **14**, 3733 (1981).
- ²⁰H. Feshbach, *Ann. Phys.* **5**, 357 (1958); **19**, 287 (1962).
- ²¹Y. Hahn, *Phys. Rev. A* **12**, 895 (1975).
- ²²M. S. Pindzola, A. Temkin, and A. K. Bhatia, *Phys. Rev. A* **19**, 72 (1979).
- ²³W. T. Rogers, G. Stefani, R. Camilloni, G. H. Dunn, A. Z. Msezane, and R. J. W. Henry (unpublished).
- ²⁴N. F. Mott and H. S. W. Massey, *The Theory of Atomic Collisions* (Oxford University Press, Oxford, 1965).
- ²⁵K. J. LaGattuta and Y. Hahn, *Phys. Rev. A* **24**, 2273 (1981).
- ²⁶H. P. Kelly and R. L. Simons, *Phys. Rev. Lett.* **30**, 529 (1973).
- ²⁷G. V. Marr and J. M. Austin, *J. Phys. B* **2**, 107 (1969).
- ²⁸A. Hashizume and N. Wasada, *Jpn. J. Appl. Phys.* **18**, 429 (1979).
- ²⁹C. G. Back, M. D. White, V. Pejcev, and K. J. Ross, *J. Phys. B* **14**, 1497 (1981).
- ³⁰C. F. Fisher, *Comput. Phys. Commun.* **1**, 151 (1969).
- ³¹J. H. Miller, R. L. Chase, A. W. Fliflet, G. R. Daum, S. L. Carter, and H. P. Kelly (unpublished).
- ³²E. J. McGuire, *Phys. Rev. A* **16**, 62 (1977); *Phys. Rev. A* **16**, 73 (1977).
- ³³R. D. Cowan and D. C. Griffin, *J. Opt. Soc. Am.* **66**, 1010 (1976).
- ³⁴J. P. Desclaux, *Comp. Phys. Commun.* **9**, 31 (1975).
- ³⁵C. F. Fisher, *J. Phys. B* **10**, 1241 (1977); *Phys. Scr.* **21**, 525 (1980).
- ³⁶K. Jonkowski, P. Malinowski, and J. Palasik, *J. Phys. B* **12**, 345 (1979).
- ³⁷M. E. Riley and D. G. Truhlar, *J. Chem. Phys.* **63**, 2182 (1975).
- ³⁸R. E. H. Clark, N. H. Magee, Jr., J. B. Mann, and A. L. Merts (unpublished).
- ³⁹The atomic structure program is described in R. D. Cowan, *The Theory of Atomic Structure and Spectra* (University of California Press, Berkeley, 1981).